Proceedings of the 7th World Congress on Momentum, Heat and Mass Transfer (MHMT'22)
~~Lisbon, Portugal~~ Virtual Conference – April 07 – 09, 2022
Paper No. ICMFHT 172
DOI: 10.11159/icmfht22.172

A Study on the Mathematical Modelling of Homogeneous Condensation in Supersonic Separators

Nathalia Sa[1,2], Antonio O S Moraes[1,2], Pedro Kropf[2], Ricardo Medronho[1], Luiz F L R Silva[1], Tânia Klein[1], Fabio Santos[1]

[1] LabCFD, Departamento de Engenharia Química, Escola de Química, Universidade Federal do Rio de Janeiro
Centro de Tecnologia, Bloco K, Ilha do Fundão, Rio de Janeiro-RJ, 21945-970, Brazil
[2]WIKKI Brasil Consultoria em Engenharia LTDA.
Parque Tecnológico da UFRJ, Rio de Janeiro, RJ, 21941-907, Brazil
nathacsa@eq.ufrj.br

Abstract **–** As the need to treat multicomponent gaseous mixtures persists in many industrial fields, supersonic separators have been gaining visibility as a viable option for removing contaminants that are difficult to isolate through conventional means. However, those separators are still not broadly studied, and much is yet to be understood about their optimal design to maximize efficiency. A detailed comprehension of the condensation phenomenon is one of the milestones to be crossed, as both homogeneous and heterogeneous condensation can occur, which makes the complete mathematical modelling of all the physics in place more complex. Using Computational Fluid Dynamics (CFD), the present work seeks to establish a robust model for the homogeneous condensation in a supersonic separator without compromising computational costs. The proposed model was based on previous works from the literature. It was implemented in OpenFOAM® software framework, and the numerical results were compared to available experimental data.

Keywords**:** supersonic, condensation, nozzle, separation, simulation, CFD

1. Introduction

There are several industrial processes where a gas mixture must be purified to separate the component of interest from one or more contaminant components. A good example is natural gas production from underground reservoirs. This natural gas usually contains hydrocarbons heavier than the C1-C2 fractions and a significant concentration of carbon dioxide (CO_2). This last contaminant is especially crucial to be removed, as it can cause issues such as corrosion and formation of hydrates, aside from the importance of preventing its emissions to the atmosphere [1]. CO_2 separation from natural gas, however, is not trivial. Techniques such as adsorption, absorption or membrane separation can be expensive, generate more effluents and require extensive installations that would be unpractical in places like oil platforms and FPSO, where primary treatment of the natural gas produced is needed.

Supersonic separators may be a viable alternative because of their simple design. In such device, a high-pressure gas stream is induced into a swirling flow and choked through a nozzle, leading to the condensation of CO_2. The newly formed droplets are captured in a thin liquid film at the walls due to the high swirl velocity. The liquid film then flows along the walls and is collected in the divergent section of the separator, and the dry gas leaves the main nozzle [2]. The process is shown in Figure 1.

Computational Fluid Dynamics (CFD) tools are employed to aid the design process of the apparatus. Parameters like the diameter and position of the throat, the ratio of inlet to throat diameter, length of the divergent section, among others, all affect the separator performance, making it imperative that each proposed geometry is tested and optimized. In order to reproduce the physics of a supersonic separator in a numerical simulation, the phenomena taking place in its interior must be adequately represented. These include, among others, condensation itself, re-evaporation caused by the expansion, turbulence in chokes, particle-wall and particle-particle interactions and the flow rate of liquid at the outlet [1]. Such effects are not trivial to model simultaneously.

Thus, simulation efforts began focusing on single-phase flows to understand the overall behaviour of the multicomponent mixture across the equipment. Malyshikna [3] and Alnoush and Castier [4], for example, represented flows as a single-phase to obtain pressure and temperature profiles caused by the choke. Some works started applying a Lagrangean approach to account for the effects of condensed droplets in the domain, but more accurate characterization of the process requires the consideration of droplet nucleation, growth, coalescence, rotation and wall collision [1][2]. Some works have recently emerged with that purpose, like the ones from Ding et al. [1] and Wen et al. [2], although computational costs and numerical stability are still a concern in current developments, as both works used a multifluid model to describe the multiphase flow.

Therefore, the present work presents the development of a solver for the CFD package OpenFOAM®, called *homogeneousCondensationFoam*, which can accurately predict the thermo-fluid dynamic behaviour inside a supersonic separator with low simulation times, considering the effects of homogeneous condensation and swirling using a simplified multiphase approach.

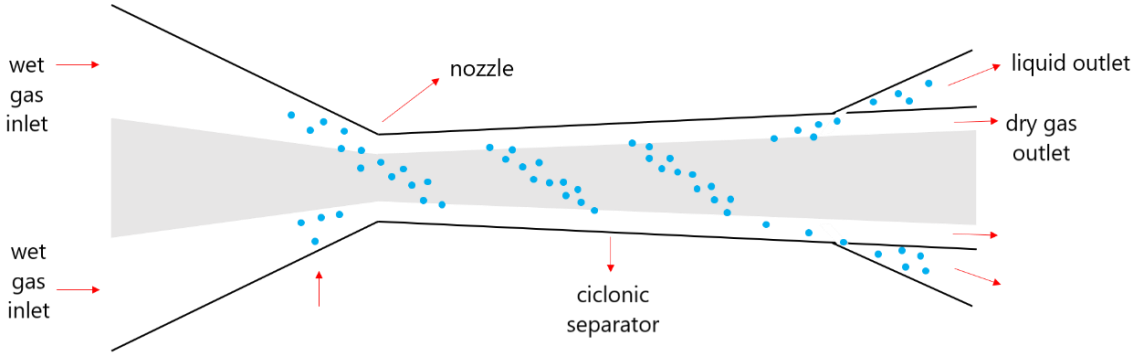

Fig. 1: Schematization of a supersonic separator.

2. Mathematical model

The multiphase flow is described by a simplified mixture model, which neglects the slip effects between phases and considers that the gas phase completely absorbs the latent heat released due to condensation. Moreover, only the condensation is considered in the present model, i.e., drops re-evaporation was not considered. Thus, Eqs. (1) - (3) are the transport equations for the gas (continuous) phase:

$$\frac{\partial \rho}{\partial t} + \nabla \cdot (\rho\, \mathbf{u}) = -\dot{m}_{vl} \quad , \tag{1}$$

$$\frac{\partial (\rho\, \mathbf{u})}{\partial t} + \nabla \cdot (\rho\, \mathbf{u} \otimes \mathbf{u}) = -\nabla p + \rho \mathbf{g} + \nabla \cdot \boldsymbol{\tau}_{eff} - \dot{m}_{vl}\mathbf{u} - \mathbf{2/3}\nabla \cdot (\rho\kappa\boldsymbol{\delta}) \quad , \tag{2}$$

$$\frac{\partial (\rho\, h)}{\partial t} + \nabla \cdot [\rho \mathbf{u}(h + K)] = \nabla \cdot (\lambda_{eff}\, \nabla T) + \frac{Dp}{Dt} + \nabla \cdot (\boldsymbol{\tau_{eff}} \cdot \mathbf{u}) - 2/3\nabla \cdot (\rho\kappa\mathbf{u}) + \dot{m}_{vl}(L - h) \ , \tag{3}$$

where $\mathbf{u}$ is the velocity vector, p is the pressure, $\mathbf{g}$ is the gravity acceleration vector, κ is the turbulent kinetic energy, λ_{eff} is the effective thermal conductivity, and L is the latent heat of vaporization for the liquid. The Dirac delta is represented by $\boldsymbol{\delta}$.The $\dot{m}_{vl}$ term represents the mass sources due to condensation, while $\dot{m}_{vl}\mathbf{u}$ and $\dot{m}_{vl}(L\text{-}h)$ are its associated momentum and energy sources, respectively. The enthalpy h and kinetic energy K are also representative of the whole domain occupied by both phases and not one phase individually, as well as the temperature T. The species mass fractions (w_i) conservation is given by Eq. (4), where ν and Sc are the kinematic viscosity and Schmidt number respectively, making ν_t and Sc_t the turbulent viscosity and Schmidt numbers, respectively:

$$\frac{\partial (\rho\, w_i)}{\partial t} + \nabla \cdot [\rho\, \mathbf{u} w_i] = \nabla \cdot \left[\left(\frac{\mu}{\rho Sc} + \frac{\nu_t}{Sc_t}\right) \nabla w_i\right] - \dot{m}_{vl} \quad , \tag{4}$$

being the density (ρ) and viscosity (μ) of the multicomponent mixture in the gas phase were calculated by Eqs. (5)-(6):

$$\rho = \sum_{i}^{n} \rho_i w_i \quad , \tag{5}$$

$$\mu = \sum_{i}^{n} \mu_i w_i \quad , \tag{6}$$

The Reynolds tensor from Eq. (2) and (3) is calculated through the RANS approach, as given by Eq. (7) below.

$$\tau_{eff_{ij}} = -(\mu + \mu_t)\left[\left(\frac{\partial u_j}{\partial x_i} + \frac{\partial u_i}{\partial x_j}\right) - \frac{2}{3}\frac{\partial u_k}{\partial x_k}\delta_{ij}\right] \quad , \tag{7}$$

where the two-equation κ-ω SST model was employed to calculate the turbulent viscosity (μ_t) [5][6][7].

2.1. Homogeneous condensation

The mass source is obtained through the classic theory of nucleation. As proposed by Wen et al. [2], the nucleation rate *J* can be calculated as shown in Eq. (8):

$$J = \frac{q_c}{1+\phi}\frac{\rho^2}{\rho_l}\sqrt{\frac{2\sigma}{\pi m_{vl}^3}}\; exp\left(-\frac{4\pi\sigma}{3k_B T}r_c^2\right) , \tag{8}$$

where $q_c = 1$ is a constant, σ is the surface tension, k_B is the Boltzmann constant, ρ_l represents liquid phase density and the ϕ factor is given by Eq. (9) below.

$$\phi = 2\frac{\gamma-1}{\gamma+1}\frac{L}{RT}\left(\frac{L}{RT} - \frac{1}{2}\right) \quad , \quad \gamma = \frac{C_p}{C_v} \quad , \tag{9}$$

where *R* is the universal gas constant, C_p and C_v are the specific heat capacities at constant pressure and volume, respectively. The critical nucleation radius, r_c, which appears in Eq. (7), represents the initial size of the particles generated by nucleation and is calculated by Eq. (10) below:

$$r_c = \frac{2\sigma}{\rho_l RT \ln S} \quad . \tag{10}$$

S is the oversaturation given by Eq. (11) below:

$$S = \frac{p_v}{p_{sat}(T)} \quad , \tag{11}$$

with p_v representing the partial pressure of the condensable component in the gaseous mixture and p_{sat} its saturation pressure at temperature *T*. The partial pressure is obtained through Dalton's Law shown in Eq. (12), using the molar fraction of condensable vapor at the gas phase, y_c, calculated from the mass fraction and molar mass M_c. The saturation pressure is calculated by Antoine's Equation, Eq. (13).

$$p_v = y_c p \quad , \quad y_c = \frac{w_c/M_c}{\sum_i w_i/M_i} \quad , \tag{12}$$

$$\log p_{sat} = A + \frac{B}{T + C} \quad . \tag{13}$$

Particle growth rate, expressed by the temporal variation of its radius r_d, is given by Eq. (14). It is a function of the phase conductivity k, the Knudsen number, K_n, the Prandtl number Pr, and adjustable parameter $\beta = 0$ and υ is a correction factor given by Eq. (15), where $a = 1$ is another adjustable parameter:

$$\frac{dr_d}{dt} = \frac{k\,[T_{sat}(p_v) - T]}{\rho_l\, L\, r_d} \frac{(1 - r_c/r_d)}{\left[\frac{1}{1 + 2\beta K_n} + 3.78(1 - \upsilon)\frac{K_n}{Pr}\right]} \quad , \tag{14}$$

$$\upsilon = \frac{RT_{sat}}{L}\left[a - 0.5 - \frac{2 - q_c}{2q_c}\left(\frac{\gamma + 1}{2\gamma}\right)\left(\frac{C_p T_{sat}}{L}\right)\right] \quad . \tag{15}$$

The final expression for the condensation rate is then given by Eq. (16) below:

$$\dot{m}_{vl} = \frac{4\pi r_c^3}{3}\rho_l J + 4\pi r_d^2 \rho_l N \frac{dr_d}{dt} \quad , \tag{16}$$

where N is the concentration of particles per unit volume, related to J by Eq. (17):

$$\frac{\partial N}{\partial t} + \nabla \cdot (N\,\mathbf{u}) = J \tag{17}$$

Finally, the radius of a particle r_d is calculated by Eq. (18) using the variable W, which represents the generated pseudo liquid component mass fraction transported through the domain, as characterized by Eq. (19).

$$r_d = \left(\frac{3W}{4\pi N}\right)^3 \quad , \tag{18}$$

$$\frac{\partial(\rho W)}{\partial t} + \nabla \cdot (\rho W\,\mathbf{u}) = \dot{m}_{vl} \quad . \tag{19}$$

3. Methodology

The mathematical model described in the previous section was implemented in OpenFOAM® v21.06. The new solver, *homogeneousCondensationFoam*, was used alongside the κ-ω SST turbulence model to simulate the experiments from Wyslouzil et al. [8], consisting of a moist nitrogen flow stream through a 2D Laval nozzle. The stagnation pressure at the inlet is fixed at p_{in} = 60 kPa and the temperature at T_{in} = 13.5ºC. The partial pressure of water was fixed at three different values: 0.26, 0.5 and 1.0 kPa.

A planar two-dimensional computational mesh with 5760 hexahedral elements was built with Pointwise® software and is shown in Figure 2. The thermophysical properties for the phases were all set to vary with temperature, with gas densities given by Ideal Gas Law, viscosities calculated from Sutherland's equation and both surface tension and heat capacities obtained from polynomial functions of T. The reference latent heat of vaporization of L_0 = 40,66 kJ/mol [8] was used to obtain the latent heat as a function of temperature through Watson's equation, Eq. (20) shown below.

$$L = L_0\left[\frac{1 - T_r}{1 - T_{br}}\right]^n \quad , \tag{20}$$

where T_r is the reduced temperature for the liquid and T_{br} is the reduced boiling temperature for the liquid. As for numerical schemes, the PIMPLE (merged SIMPLE-PISO algorithm) algorithm from OpenFOAM® was used to solve the coupled system of transport equations in a segregated manner. The *localEuler* scheme as implemented in OpenFOAM® was used for the time derivative discretization, while the second order upwind scheme is used for the divergence operator discretization. The *localEuler* scheme is a pseudo-transient method based on using a local time scale approach to achieve the steady-state condition.

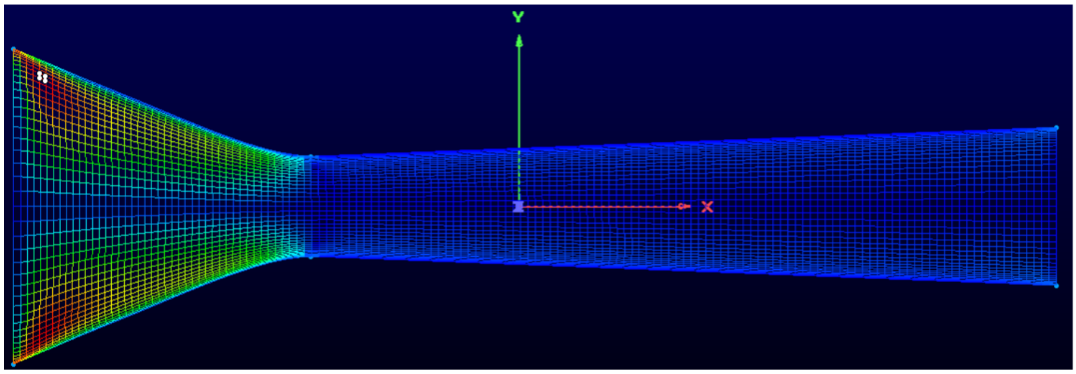

Fig. 2: Computational mesh.

For boundary conditions, the *totalPressure* and *totalTemperature* boundary conditions as implemented in OpenFOAM® were employed at the inlet, which make isentropic corrections for gases considering the Mach number (*Ma*). For the outlet, a *waveTransmissive* condition is used to avoid the reflection of shockwaves at the boundary.

4. Results and Discussion

Figure 3 shows the comparison between simulations and the experimental data from Wyslouzil et al. [8]. It is noticeable how the model is able to predict the pressure profile inside the separator for each inlet condition. The dry case, corresponding to a simulation of pure nitrogen, is included to illustrate the effect of condensation over the shock. The results still show some discrepancy regarding the exact position where the onset of condensation occurs, which is predicted in the simulations to be earlier than the experimental data determines.

As for the homogeneous condensation variables, Figure 4 shows contours of nucleation rate (J), oversaturation (S), condensation rate ($\dot{m}$) and particle radius (r_d) along the domain. Figure 5 shows the plot of those same variables along the centerline of the nozzle. It can be seen that, as expected, nucleation occurs right after the throat and droplet growth increases after this region. Condensation rates diminish as the divergent section diameter increases. Figure 6 shows the decline in water mass fraction (w_{H2O}) inside the gas phase along the nozzle length. Shortly after the throat, indicated by $L = 0$ *mm* in Figures 4 to 6, the contents of H_2O in the gas phase start declining, and the liquid water phase mass fraction starts increasing.

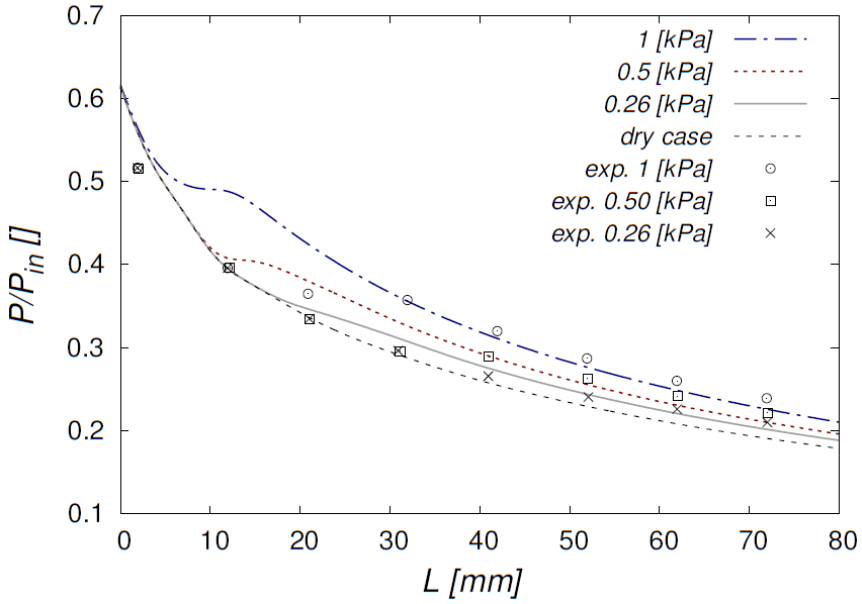

Fig. 3: Comparison of simulation results to experimental data [8] for pressure profile.

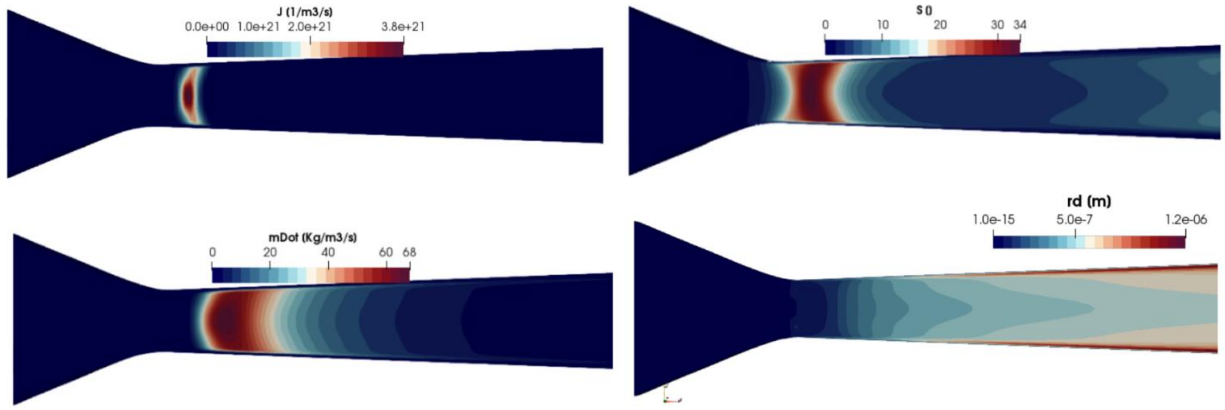

Fig. 4: Contours of nucleation rate J (top left), oversaturation S (top right), condensation rate $\dot{m}$ (bottom left) and droplet radius r_d (bottom right).

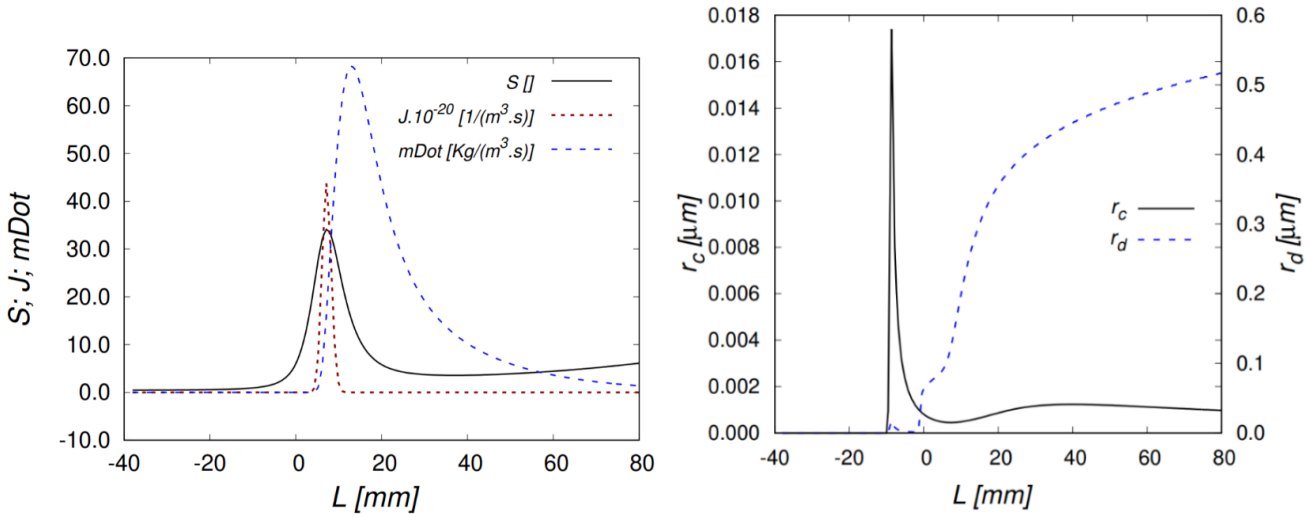

Fig. 5: Centerline profiles of nucleation rate J, oversaturation S and condensation rate $\dot{m}$ (left) and comparison between droplet radius r_d and its critical initial value r_c (right). The nozzle throat is at position $L = 0$ *mm*.

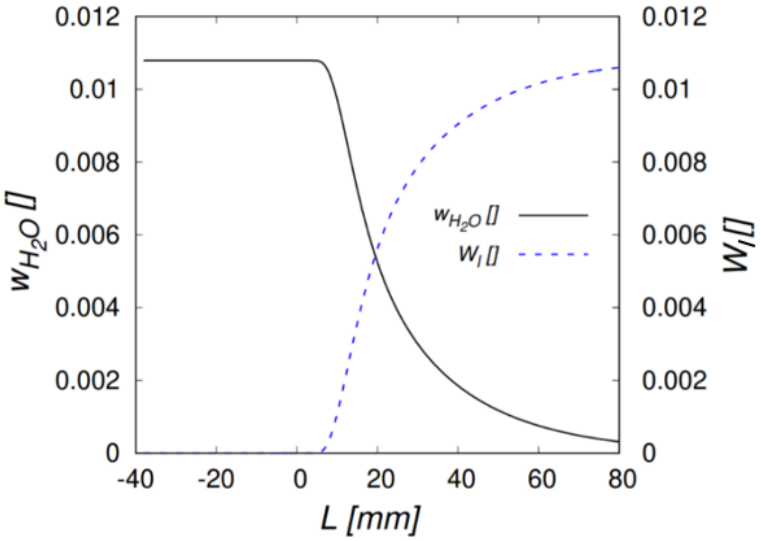

Fig. 6: Centerline profiles of steam mass fraction in the gas phase (w_{H2O}) and liquid fase mass fraction (W_l). The nozzle throat is at position $L = 0$ *mm*.

5. Conclusion

The implemented homogeneous condensation model for a mixture multiphase simulation proved to be promising in characterizing the flow inside a supersonic separator. Experimental profiles of pressure and temperature from Wyslouzil et al. [8] were captured with a good agreement, and the solver *homogeneousCondensationFoam* required less computational power than multifluid solvers, providing faster results with numerical stability. Future works can now focus on more practical designs of supersonic separators, also including the study of the effects of liquid collectors in the geometry.

Acknowledgements

The authors would like to thank Petrobras S.A. for funding the project.

References

[1] H. Ding, C. Sun, C. Wang, C. Wen, and Y. Tian. *Prediction of dehydration performance of supersonic separator based on a multifluid model with heterogeneous condensation*. Applied Thermal Engineering, vol. 171, pp. 115074, 2020.

[2] C. Wen, N. Karvounis, J. H. Walther, Y. Yan, Y. Feng, and Y. Yang. *An efficient approach to separate CO_2 using supersonic flows for carbon capture and storage*. Applied Energy, vol. 238, pp. 311–319, 2019.

[3] M. Malyshkina. *The procedure for investigation of the efficiency of purification of natural gases in a supersonic* separator. High Temperature, vol. 48, no. 2, pp. 244–250, 2010.

[4] W. Alnoush, M. Castier. *Shortcut modelling of natural gas supersonic separation*. Journal of Natural Gas Science and Engineering, vol. 65, pp. 284–300, 2019.

[5] F. R. Menter and T. Esch. *Elements of Industrial Heat Transfer Prediction*. 16th Brazilian Congress of Mechanical Engineering (COBEM), 2001.

[6] F. R. Menter, M. Kuntz and R. Langtry. Ten Years of Industrial Experience with the SST Turbulence Model. Turbulence, Heat and Mass Transfer 4, ed: K. Hanjalic, Y. Nagano & M. Tummers, Begell Houde, Inc., 625-632, (2003).

[7] A. Hellsten. *Some Improvements in Menter's k-omega-SST turbulence model*. 29th AIAA Fluid Dynamics Conference, AIAA-98-2554, 1998.

[8] B. E. Wyslouzil, C. H. Heath, J. L. Cheung, and G. Wilemski. *Binary condensation in a supersonic nozzle*. The Journal of Chemical Physics, vol. 113, no. 17, pp. 7317–7329, 2000.

[9] J. Young. *The spontaneous condensation of steam in supersonic nozzle*. Physico Chemical Hydrodynamics, vol. 3, pp. 57–82, 1982.

[10] J. H. Ferziger and M. Perić. Computational Methods for Fluid Dynamics. Springer, Germany,2nd Edition, 1997.

[11] F. Moukalled, L. Mangani, and M. Darwish. The Finite Volume Method in Computational Fluid Dynamics. Springer, 2015.